Large Slip Effect at a Nonwetting Fluid-Solid Interface

Jean-Louis Barrat
Département de Physique des Matériaux, Université Claude Bernard and CNRS, 69622 Villeurbanne Cedex, France

Lydéric Bocquet
Laboratoire de Physique, ENS-Lyon and CNRS, 69364 Lyon Cedex 07, France
(Received 13 November 1998)

It is well known that, at a macroscopic level, the boundary condition for a viscous fluid at a solid wall is one of "no slip." The liquid velocity field vanishes at a fixed solid boundary. We consider the special case of a liquid that partially wets the solid (i.e., a drop of liquid, in equilibrium with its vapor on the solid substrate, has a finite contact angle). Using extensive molecular dynamics simulations, we show that when the contact angle is large enough, the boundary condition can drastically differ (at a microscopic level) from a no-slip condition. Slipping lengths exceeding 30 molecular diameters are obtained for a contact angle of 140°, characteristic of mercury on glass. This finding may have important implications for the transport properties in nanoporous media under such "nonwetting" conditions. [S0031-9007(99)09329-1]

PACS numbers: 68.15.+e, 61.20.Ja, 68.45.Gd

Properties of confined liquids have been the object of constant interest during the last two decades, thanks to the considerable development of surface force apparatus techniques. While static properties are now rather well understood (see, e.g., [1]), the dynamics of confined systems have been investigated more recently [2]. These studies have motivated much numerical and theoretical work [3–8] and some progress has been made in giving a simple coherent description of the collective dynamics of confined liquids. Both from experimental and theoretical studies has emerged a rather simple description of the dynamics of not too thin liquid films—i.e., films thicker than typically 10 to 20 atomic sizes. The hydrodynamics of the film can be described by the macroscopic hydrodynamic equations with bulk transport coefficients, supplemented by a "no-slip" boundary condition applied in the vicinity (i.e., within one molecular layer) of the solid wall. Hence, in spite of the fact that the wall induces a layering of the fluid that can extend 5 to 6 molecular diameters from the wall, the hydrodynamic properties of the interface are quite simple.

It turns out, however, that all experimental and numerical studies of confined fluids have been carried out with fluid/substrate combinations that correspond to a total wetting situation. By this we mean that $\gamma_{LS} + \gamma_{LV} < \gamma_{SV}$, where γ is an excess surface free energy and the indexes L, V, and S refer, respectively, to the liquid, its vapor, and the substrate [9]. In this Letter, we investigate the structure and the hydrodynamic properties of a fluid film that is forced to penetrate a narrow pore in a situation of partial wetting, i.e., when $\gamma_{LS} + \gamma_{LV} > \gamma_{SV}$. This condition corresponds to the case where a drop of the liquid resting on the same substrate, at equilibrium with its vapor, has a finite contact angle θ which can be deduced from Young's law $\gamma_{LV} \cos\theta = (\gamma_{SV} - \gamma_{LS})$ [10].

We first describe our model for the fluid and the substrate, and some details of the simulation procedure. All interactions are of the Lennard-Jones type,

$$v_{ij}(r) = 4\epsilon\left[\left(\frac{\sigma}{r}\right)^{12} - c_{ij}\left(\frac{\sigma}{r}\right)^{6}\right] \qquad (1)$$

with identical interaction energies and molecular diameters σ. The surface energies will be adjusted by tuning the coefficients c_{ij}. In all the simulations that are presented in this Letter, the solid substrate is described by atoms fixed on a fcc lattice, with a reduced density $\rho_S\sigma^3 = 0.9$. As the wall atoms are fixed, the coefficient c_{SS} is in fact irrelevant. The interactions between fluid atoms are characterized by $c_{FF} = 1.2$, meaning that the fluid under study is more cohesive than the usual Lennard-Jones fluid. The fluid-substrate interaction coefficient c_{FS} will be varied between 0.5 and 1. All the simulations will be carried out at a constant reduced temperature, $k_BT/\epsilon = 1$.

The configuration under study will be a fluid slab confined between two parallel solid walls. Typically, a configuration contains 10 000 atoms, with a distance between solid walls $h = 18\sigma$ and lateral cell dimensions $L_x = L_y = 20\sigma$. Periodic boundary conditions are applied in the x and y directions, i.e.y parallel to the walls. For each wall, three layers of fcc solid (in the 100 orientation) will be modeled using point atoms, a continuous attraction between the fluid and the wall in the direction perpendicular to the walls being added in order to model the influence of the deeper solid layers. All simulations were carried out at constant temperature ($k_BT/\epsilon = 1$) by coupling the fluid atoms to a Hoover's thermostat [11]. In flow experiments, only the velocity component in the direction orthogonal to the flow was thermostated.

Before we discuss in detail the structure of a film, we can roughly estimate the influence of the interaction

parameters on the wetting properties of the fluid. Following the standard Laplace estimate of surface energies [10], we have $\gamma_{ij} \simeq -\rho_i \rho_j \int_{r_0}^{\infty} r u_{ij}(r)\, dr$. Using Young's law, we obtain for the contact angle $\cos\theta = -1 + 2\rho_S c_{FS}/\rho_F c_{FF}$.

From this expression, a variation of c_{FS} between 0.5 and 0.9 would be expected to induce a variation of θ between 100° and 50°. A more accurate determination of the surface tensions was carried out using the method of Nijmeijer *et al.* [12]. The surface tensions are defined in terms of an integral over components of the pressure tensors which can be computed in a simulation. We refer to Ref. [12] for more details. By tuning the solid-fluid interaction strength c_{FS} from $c_{FS} = 1.0$ to $c_{FS} = 0.5$, we found the contact angle deduced from Young's law varies from $\theta \simeq 90°$ to $\theta \simeq 140°$. In Fig. 1, a typical configuration of a liquid droplet (in coexistence with its vapor) on the solid substrate is shown for $c_{FS} = 0.5$, which corresponds to $\theta \simeq 140°$. The droplet was formed by starting from a liquid film of thickness 20σ, and suddenly increasing the distance between the bounding walls, so that a (metastable) liquid-vapor coexistence situation is reached. The droplet forms when some particles at the box boundary are removed, in a way that breaks the planar symetry. This picture clearly illustrates how the notion of a contact angle retains its validity down to nanometric scales [13]. In the following we shall describe such large contact angles (i.e., larger than 90°) as corresponding to a "nonwetting" situation.

In order to force the fluid into a narrow liquid pore under such partial wetting conditions, an external pressure has to be applied. A simple thermodynamic argument shows that for a parallel slit of width h, the minimal pressure is $P_0 = 2(\gamma_{LS} - \gamma_{SV})/h$. For the fluid with $c_{FS} = 0.5$, we find, for $h = 18\sigma$, $P_0 = 0.079\epsilon/\sigma^3$, while $P_0 = 0.018\epsilon/\sigma^3$ when $c_{FS} = 0.9$. If we use $\sigma = 5$ Å , $\epsilon = 0.05$ eV, then $P_0 \sim 1$ MPa for $h = 9$ nm in the nonwetting case, $\theta = 140°$.

Figure 2 shows the density profiles of the nonwetting fluid inside the pore for pressures corresponding to $2.8P_0$ and $16.4P_0$. The pressure is changed at constant pore width by changing the number of particles. It is seen in this figure that the highest pressure structure strongly resembles what would be obtained for the usual case of a wetting fluid, with a strong layering at the wall. The structure at the lower pressure is markedly different, with a strong density depletion near the wall.

We now turn to the study of the dynamical properties of the confined fluid layer. Two types of numerical experiments, corresponding to Couette and Poiseuille planar flows, were carried out. In the Couette flow experiments, the upper wall is moved with a velocity U (typically $U = 0.25-0.5$ in reduced Lennard-Jones units). In the Poiseuille flow experiment, an external force in the x direction is applied to the fluid particles. In both cases we took great care to ensure that the response of the system was linear, as it is known [14] that the boundary condition becomes nonlinear for high shear rates. In Fig. 3 and 4 we compare the resulting velocity profiles to those that would be expected for a no-slip boundary condition applied at one molecular layer from the solid wall. Obviously the velocity profiles for the nonwetting fluid imply a large amount of slip at the solid boundary. As usual, this slippage effect can be quantified by introducing a "partial slip" boundary condition for the

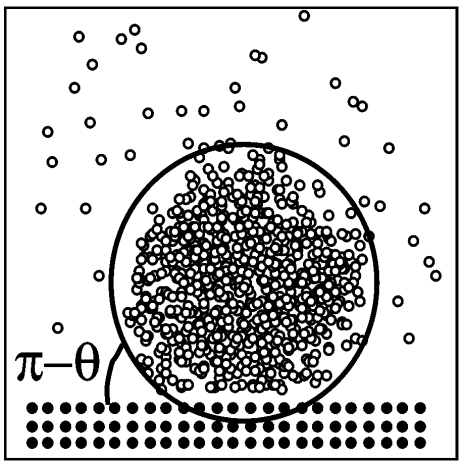

FIG. 1. A typical configuration of a liquid droplet (1000 atoms) on a solid substrate in a nonwetting case ($c_{FS} = 0.5$), in equilibrium with its vapor. This configuration was prepared by starting from a homogeneous fluid slab of thickness 18σ, confined between two walls. The droplet is formed by simultaneously moving the upper wall by 20σ in the z direction and removing the fluid atoms that lie near the box boundaries. The bounding box has a size of 20σ.

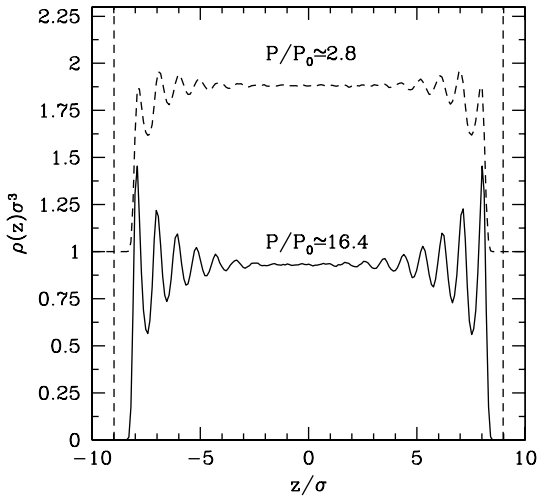

FIG. 2. Density profiles of the nonwetting fluid ($c_{FS} = 0.5$) confined between two solid walls separated by 20σ. The positions of the first layer of solid atoms have been indicated by vertical dashed lines. Full line: $P/P_0 = 16.4$; dashed line: $P/P_0 = 2.8$. The latter curve has been shifted upwards for clarity.

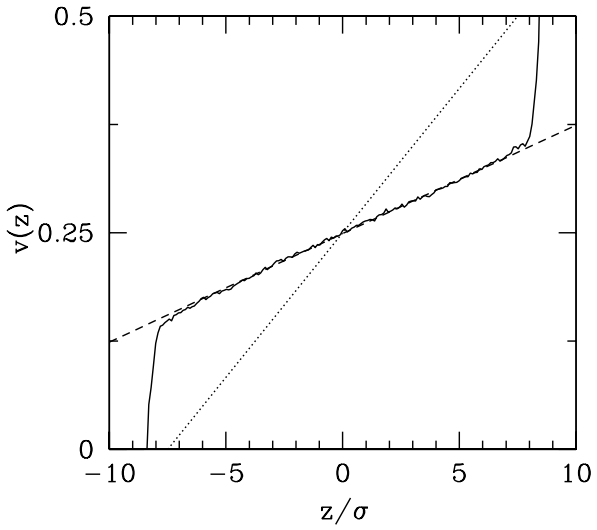

FIG. 3. Velocity profile (in reduced units) of the nonwetting fluid ($c_{FS} = 0.5$) in a Couette geometry. The reduced pressure is $P/P_0 \simeq 7.3$. The solid line is the simulation result and the dotted line is the velocity profile predicted by the no-slip boundary condition. The dashed line is the velocity profile predicted by the Navier-Stokes equations supplemented by the partial slip boundary condition, Eq. (2). The velocity of the upper wall is $U = 0.5$.

tangential velocity v_t (relative to the solid) at the solid liquid boundary. For a liquid that fills the upper half space $z > z_w$, we have

$$\frac{\partial v_t}{\partial z}|_{z=z_w} = \frac{1}{\delta} v_t|_{z=z_w} . \qquad (2)$$

This boundary condition depends on two parameters, the walllocation z_w and the slipping length δ. The usual no-slip boundary condition corresponds to the limiting case $\delta = 0$, and z_w close to the first layer of solid. When slip is present at the boundaries, the two parameters δ and z_w are obtained by fitting the profiles obtained in the simulation for the Couette and Poiseuille flow with those deduced from Eq. (2), supplemented by the usual Stokes equation in the bulk fluid. The results of such an adjustment are shown in Fig. 3 and 4. In these figures, it can be seen that this procedure gives an extremely good fit to the flow profile in the slab, allowing an accurate determination of δ and z.

It turns out that, as was the case in earlier studies [6], the hydrodynamic position z_w of the walls is located inside the fluid, typically one atomic distance from the outer layer of solid atoms. As a consequence, δ can be obtained simply as the distance within the solid at which the extrapolated velocity of the fluid relative to the solid would vanish, taking as an origin the $z = z_w \simeq \pm 9\sigma$ plane. In earlier work, this distance was always found to be very small (typically less than one atomic size for such simple fluids; see, however, [14]). In Fig. 5, the variation of δ as a function of the pressure is shown for several values of the interaction parameters. The pressure is normalized by the capillary pressure P_0 defined above as the minimal pressure that must be applied to the fluid in order to enter the pore. For an interaction parameter $c_{FS} = 0.9$, corresponding to a contact angle $\theta = 100°$, the usual behavior (i.e., a small δ) is obtained. For an interaction parameter $c_{FS} = 0.5$ which corresponds to a contact angle $\theta = 150°$ [15], slipping lengths larger than 15 molecular diameters can be obtained at the lowest pressures; even at relatively high pressures ($10P_0$), the slipping length remains appreciably larger than the molecular size σ.

Obviously the existence of such a large slippage effect should manifest itself in the dynamical properties of a

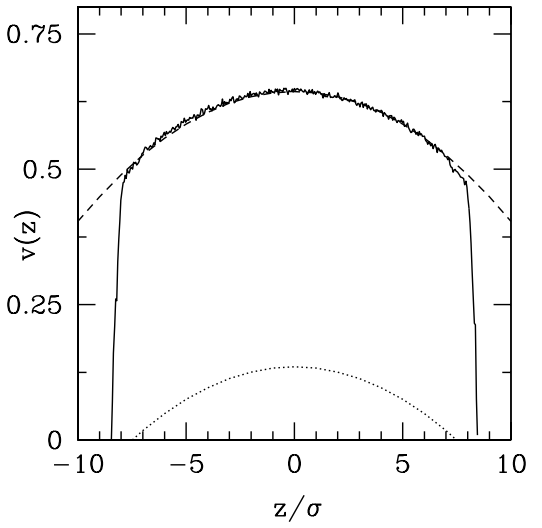

FIG. 4. Same as in Fig. 3, but in a Poiseuille geometry. The external force applied on each fluid particle is $f_{\text{ext}} = 0.02\epsilon/\sigma$.

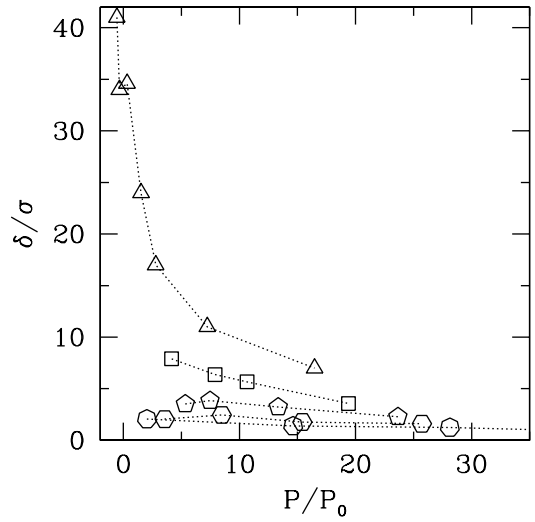

FIG. 5. Variation of the slipping length δ (in units of σ) as a function of the reduced pressure P/P_0, for several values of the interaction parameters c_{FS}. From top to bottom, the data correspond to $c_{FS} = 0.5$, $c_{FS} = 0.6$, $c_{FS} = 0.7$, $c_{FS} = 0.8$, $c_{FS} = 0.9$. Dotted lines are a guide for the eye.

liquid confined in a nanoporous medium. The essential parameter that characterizes a porous medium is its permeability, which relates the flow rate to the pressure drop [16] across the medium. This permeability is proportional to the permeability of a single capillary, with a proportionality factor that depends on the geometrical characteristics of the medium. If one considers a single cylindrical capillary, a straightforward calculation in the Poiseuille geometry shows that the existence of slip on the boundaries increases the flow rate in the tube as compared to the "usual" no-slip case by a factor $1 + 8\delta/h$ (with h the pore diameter and δ the slip length). Thus, in a porous medium, the effective permeability K_{eff} is expected to increase by the same factor, i.e., $K_{\text{eff}} = K_0(1 + 8\frac{\delta}{h})$, where K_0 is the "standard" permeability, obtained within the no-slip assumption. In a wetting situation, δ is found to be very small and $K_{\text{eff}} \simeq K_0$. However, in a nonwetting situation ($\theta \sim 140°$), the slipping length δ may largely exceed the nanometric pore sizes h, so that the effective permeability K_{eff} is expected to be much larger than K_0 (say, more than 1 order of magnitude in view of the prefactors). In fact, it is quite likely that the decrease in the "apparent viscosity" observed by Churaev and co-workers [17] in their studies of flow of mercury in micrometric capillaries could be ascribed to this effect. It can also be expected that the microscopic dynamics of the molecules could be rather different in a nonwetting medium, compared to what it is in the bulk or in a medium with strong solid/liquid affinity. In fact, recent studies point towards the importance of the surface treatment for the reorientation dynamics of small molecules in nanopores [18]. Correlating the wetting properties with such microscopic studies seems to be a promising area for future research.

This work was supported by the Pole Scientifique de Modélisation Numérique at ENS-Lyon, the CDCSP at the University of Lyon, the DGA and the French Ministry of Education under Contract No. 98/1776. We thank E. Charlaix and P.-F. Gobin for introducing us to this subject, and Dr. S. J. Plimpton for making publicly available a parallel MD code [19], a modified version of which was used in the present simulations. We also thank R. Pit for pointing out Ref. [17] to us.

[1] J. N. Israelachvili, *Intermolecular and Surface Forces* (Academic Press, London, 1985).

[2] *Dynamics in Small Confining Systems*, edited by J. M. Drake, J. Klafter, and R. Kopelman (MRS, Pittsburgh, 1996); J. N. Israelachvili, P. M. McGuiggan, and A. M. Homola, Science, **240**, 189 (1988); H. W. Hu, G. A. Carson, and S. Granick, Phys. Rev. Lett. **66**, 2758 (1991); J.-M. Georges, S. Millot, J.-L. Loubet, and A. Tonck, J. Chem. Phys. **98**, 7345 (1993).

[3] J. Koplik, J. R. Benavar, and J. F. Willemsen, Phys. Rev. Lett. **60**, 1282 (1988).

[4] P. A. Thompson and M. O. Robbins, Phys. Rev. A **41**, 6830 (1990).

[5] I. Bitsanis, S. A. Somers, H. T. Davis, and M. Tirrell, J. Chem. Phys. **93**, 3427 (1990).

[6] L. Bocquet and J.-L. Barrat, Phys. Rev. E **49**, 3079 (1994); J. Phys. Condens. Matter **8**, 9297 (1996).

[7] C. J. Mundy, S. Balasubramanian, K. Bagchi, J. I. Siepmann, and M. L. Klein, Faraday Discuss. **104**, 17 (1996).

[8] J. Koplik and J. R. Banavar, Phys. Rev. Lett. **80**, 5125 (1998).

[9] We mention that in some numerical simulations, purely repulsive interactions between the fluid and the substrate were considered. In that case, however, the pressure of the fluid is very high, and the properties of the confined fluid is very similar to what is obtained for a wetting fluid (with attractive interactions to the substrate) at a lower pressure.

[10] J. S. Rowlinson and B. Widom, *Molecular Theory of Capillarity* (Oxford University Press, Oxford, 1989).

[11] M. Allen and D. Tildesley, *Computer Simulation of Liquids* (Oxford University Press, Oxford, 1987).

[12] M. J. P. Nijmeijer, C. Bruin, A. F. Bakker, J. M. J van Leeuwen, Phys. Rev. A **42**, 6052 (1990).

[13] J. Hautman *et al.*, Phys. Rev. Lett. **67**, 1763 (1991).

[14] P. A. Thompson and S. M. Troian, Nature (London) **389**, 360 (1997). In this paper it was observed that at high shear rates a large slipping length can appear due to nonlinear effects. The shear rates used in the present work, however, are typically 1 order of magnitude lower than those at which the nonlinear increase of δ was observed by Thompson and Troian.

[15] The contact angle of mercury on glass is typically 140°.

[16] J. Bear, *Dynamics of Fluids in Porous Media* (Elsevier, New York, 1972).

[17] M. V. Churaev, V. D. Sobolev, and A. N. Somov, J. Colloid Interface Sci. **97**, 574 (1984).

[18] M. Arndt, R. Stannarius, W. Gorbatschow, and F. Kremer, Phys. Rev. E **54**, 5377 (1996).

[19] S. J. Plimpton, J. Comput. Phys. **117**, 1 (1995); code available at http://www.cs.sandia.gov/tech_reports/ssjplimp